Journal of Nuclear Materials 390–391 (2009) 713–716

Contents lists available at ScienceDirect

Journal of Nuclear Materials

journal homepage: www.elsevier.com/locate/jnucmat

# Calculation of deuterium retention, re-emission and reflection from a tungsten material under $D^+$ ions irradiation with ACAT-DIFFUSE code

T. Ono [a,*], T. Kenmotsu [b], T. Muramoto [a], T. Kawamura [c]

[a] Department of Computer Simulation, Faculty of Informatics, Okayama University of Science, 1-1 Ridai-cho, Okayama 700-0005, Japan
[b] Doshisha University, Tataramiyakotani 1-3, Kyotanabe-shi, Kyoto 610-0394, Japan
[c] National Institute for Fusion Science, Oroshi-cho 322-6, Toki-shi, Gifu 509-5292, Japan

ARTICLE INFO

*PACS:*
66.30-h
79.20.R
52.40.Hf
07.05.T

ABSTRACT

We calculated, with a dynamic Monte Carlo code ACAT-DIFFUSE, fluxes of thermal $D_2$ re-emission, reflection and segregated self-sputtering of D from a $D^+$ implanted wrought tungsten material during a time sequence of l00 eV $D^+$ implantation, post-implanted isothermal out-gassing and thermal desorption spectroscopy. The obtained result was in good agreement with an existing experiment if two different trap sites with de-trapping energy of 0.85 eV and 2.2 eV and density fraction of 0.05 D/W and 0.01 D/W were assumed to exist. The re-emission, reflection and self-sputtering fluxes in the implantation period were shown to be almost comparable. The integrated deuterium flux released in the same period was estimated. The amount of deuterium retained at 300 K was nearly six times higher than that at 473 K, which reflects the result that mobile atoms and atoms trapped in 0.85 eV trap existed abundantly at 300 K but scarcely at 473 K.



## 1. Introduction

A tungsten material has been selected as a candidate material of the ITER divertor plate because of its high melting temperature, good thermal conductivity and high resistive nature of erosion due to high threshold energy for sputtering [1].

The ion temperature of the boundary plasma in the ITER is estimated to be around 30 eV [2]. Many experiments [3–9] have so far studied retention, re-emission and thermal desorption spectra using ion beams with energy of hundreds of eV to a few keV, except for a few experiments which employed such low-energy ion beams [10–13].

Above issues obtained experimentally for such low-energy ions have been simulated by computer codes [10,11,13]. In the work in [13,14], a source term for the mobile atom concentration, which is given by the range distribution of implanted ions, was prescribed with a reference to the results obtained with the TRIM.SP [15]. However, as will be shown later, the concentration profiles of implanted ions were broadened out because of diffusion within the irradiation time concerned here.

In this paper, we have calculated, with a dynamic Monte Carlo code ACAT-DIFFUSE [16], fluxes of thermal $D_2$ re-emission, reflection and segregated self-sputtering of D from a $D^+$ implanted wrought tungsten material during a time sequence of l00 eV $D^+$ implantation, post-implanted isothermal out-gassing and thermal desorption spectroscopy (TDS), and compared them with above experiment [13]. We have also derived the retention and the depth distributions of deuterium retained in the material at temperatures of 300 K and 473 K. In these calculations, the radiation-enhanced diffusion of deuterium and the damage effect of trap energies were taken into account in the damage range in the code.

## 2. Simulation method

The ACAT-DIFFUSE consists of ACAT [17] part and DIFFUSE part which is based on DIFFUSE [18] code. Since the code has been introduced in detail elsewhere [16], its main features necessary to help understand the following discussions are outlined here.

A total fluence $\Phi$ is divided into smaller fluence $\Delta\Phi$ during which incident ions do not change the target composition appreciably, and ions corresponding to $\Delta\Phi$ are exposed to the target together and slowed down instantaneously. First, their slowing down and the associated vacancy and range distributions are calculated through the ACAT routine for a number of incident ions being in collisions with target atoms and previously-implanted trapped projectiles until they are thermalized to the binary collision approximation by a Monte Carlo method. Then, their thermal processes such as diffusion and recombination are treated during the time interval of $\Delta\Phi/J$ ($J$ being the ion flux), by solving a diffusion equation numerically through the DIFFUSE routine. The simulation procedure starts with a calculation of the ACAT part.

* Corresponding author.
*E-mail address:* ono@sp.ous.ac.jp (T. Ono).

0022-3115/$ - see front matter © 2009 Elsevier B.V. All rights reserved.
doi:10.1016/j.jnucmat.2009.01.196

Then, the output of the ACAT part is used as input to a calculation of the DIFFUSE part, and the output of the DIFFUSE part serves as input to the ACAT part. This iterative sequence was repeated $n$ times, where $n = \Phi/\Delta\Phi$.

Radiation-enhanced diffusion and a damage effect on the trap energy were so considered as to be proportional to the accumulated radiation damage. Since temperature concerned here was relatively low, we assumed that deuterium atoms instantly recombine with each other and leave the surface as $D_2$ when reaching the surface. We used a recombination rate coefficient $K_r = K_r^0/\sqrt{T}\exp(-E_r/kT)$ [13] with $K_r^0$ having a value $1.2\times 10^{-25}\mathrm{cm}^4\sqrt{\mathrm{K}}/\mathrm{s}$, $E_r$ activation energy for the surface recombination taken to be equal to $-0.59$ eV [19], $k$ Boltzmann constant, and $T$ temperature. Above formula for $K_r$ decreases with rising temperature, because for all endothermic materials including tungsten for hydrogen occlusion the recombination rate coefficient has the same tendency according to the theory [20]. From above assumption, released flux $J_r$ at the surface is given by:

$$J_r = K_r c_s^2 \tag{1}$$

where $c_s$ is concentration at the surface. The diffusion coefficient for deuterium atoms was employed as $D(T) = 1.0\times 10^{-8}\exp(-0.39\ \mathrm{eV}/kT)\ \mathrm{cm}^2/\mathrm{s}$, where the activation energy was taken from the work in [21]. The pre-exponential factor was a parameter in this simulation and was derived by fitting well the simulation result to the experiment. Eq. (1) offers the boundary condition at the surface for the diffusion equation.

## 3. Numerical results and discussions

We calculated fluxes of thermal re-emission of $D_2$, reflection and segregated self-sputtering of D from the $D^+$ implanted wrought tungsten in the period of implantation with 100 eV $D^+$ flux $2.0\times 10^{15}$ $D^+/\mathrm{cm}^2$ s, and flux of thermal re-emission in the out-gassing and the degassing (TDS) periods, as shown in Fig. 1, together with the experimental data [13].

Erosion of the material does not occur because the incident energy is lower than the threshold energy for sputtering (~250 eV).

The spectrum of the experimental data had two peaks at 475 K and 850 K in the TDS period. We assumed two trap sites (trap #1 and trap #2) with de-trapping energies of 0.85 eV and 2.2 eV and the density fractions of 0.05 D/W and 0.01 D/W, respectively. It is clear from the figure that the calculated result is, on the whole, in good agreement with the experimental data. The peak temperatures in the TDS period obtained were 450 K and 860 K, and close to those of the experiment cited above. The result suggests that these peaks observed by the experiment can be ascribed to the existence of the two different trap sites in the material. Since the ACAT output indicated that vacancy was hardly produced by 100 eV $D^+$ ions bombardment of tungsten to the binary collision approximation, these trap sites may have previously been created before the experiment.

The fluxes of re-emission, reflection and segregated self-sputtering show almost constant in the implantation period except for approximately early 100 s. The segregated self-sputtering indicates a large amount of deuterium had already accumulated near the surface. The ratios of these fluxes were approximately 0.45:1:0.15 relative to the reflection flux. So, it is noteworthy to point out that segregated self-sputtering of hydrogen isotopes should also be considered in assessing recycling of the first wall and the divertor plate.

Fig. 2 indicates the calculated amount of mobile and trapped deuterium atoms versus time. The amount of mobile atoms is an order of magnitude smaller than that of trapped atoms during the irradiation period. The amount of atoms held in trap #1 reaches a certain level at about 50 s after the irradiation started, and gradually decreases with time in the out-gassing period. This reduction contributes to increase the amount of mobile atoms, as depicted in the figure. Without that additional supply of mobile atoms, the flux of re-emission in the out-gassing period would have been decreased much faster than is shown in Fig. 1. On the other hand, the amount of atoms held in trap #2 keeps constant during the implantation, the out-gassing and almost the TDS periods. The sharp drop of the amount of atoms trapped in trap #1 appearing at the beginning of the TDS period results in producing the first peak of the amount of mobile atoms. The second peak is due to the decrease in the amount of atoms kept in trap #2. However, a very small portion of the de-trapped atoms falls into trap #1 again, as shown in Fig. 2. These peaks of mobile atoms, in turn, give rise to produce the two peaks of the TDS spectrum illustrated in Fig. 1.

Shown in Fig. 3 are fluxes of thermal re-emission, reflection and sputtering in the three periods calculated for the material at 473 K, which is close to the temperature (475 K) corresponding to the first peak of the TDS spectrum. The re-emission flux becomes constant a little faster than that for 300 K in the implantation period and drops drastically compared to that for 300 K and stays below $10^{10}$ $D/\mathrm{cm}^2/\mathrm{s}$ in the out-gassing period. Only one peak is seen in the TDS spectrum.

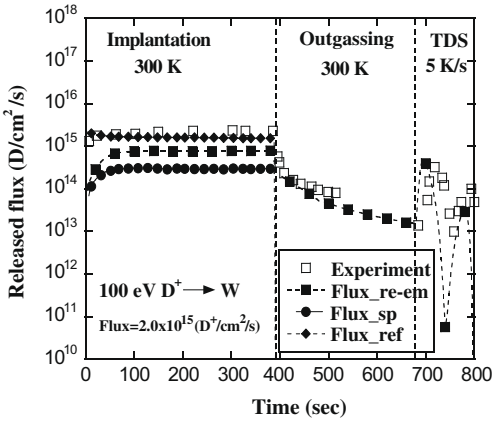


**Fig. 1.** Fluxes of thermal $D_2$ re-emission, reflection and segregated self-sputtering of D from a $D^+$ implanted wrought tungsten material during a time sequence of l00 eV $D^+$ implantation, post-implanted isothermal out-gassing and thermal desorption spectroscopy calculated with ACAT-DIFFUSE, together with the experimental result [13]. Temperature of the material was kept at 300 K in the first two periods and was raised with a ramp seed 5 K/s in the TDS period.

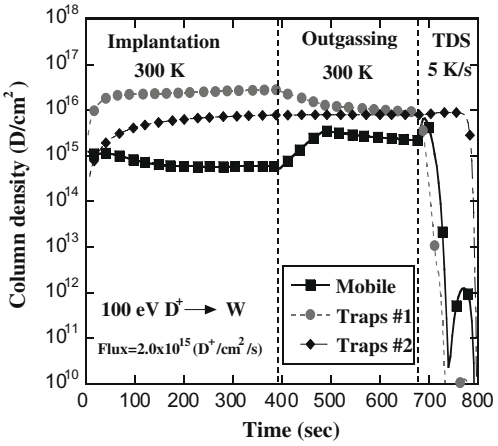


**Fig. 2.** Column density (integrated density in a cylinder 1 $\mathrm{cm}^2$ in cross section extending from the surface of the material to the bottom) of mobile deuterium atoms and trapped atoms in trap #1 and trap #2 in the case of Fig. 1.

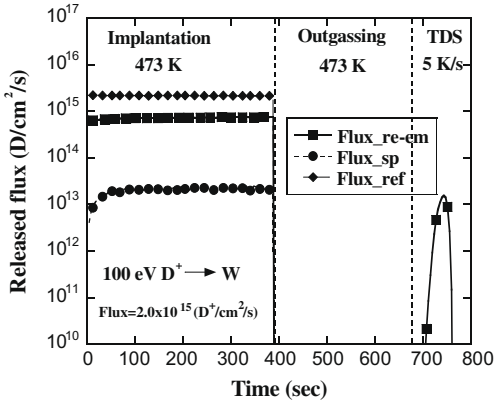


**Fig. 3.** The same fluxes as shown in Fig. 1 except the temperature 473 K in the first two periods.

Fig. 4 illustrates the calculated amount of mobile and trapped atoms at 473 K during the first two periods. From Fig. 4, it is clear that almost all atoms are trapped in trap #2 throughout the whole periods. The peak of the TDS spectrum shown in Fig. 3 can also be understood with the same explanation as above for the second peak of the TDS spectrum depicted in Fig. 1.

The amounts of deuterium atoms retained at 300 K and 473 K are shown in Fig. 5. The integrated fluxes (fluences) released at these temperatures in the implanted period were estimated to be $7.49 \times 10^{17}$ D/cm$^2$ and $7.78 \times 10^{17}$ D/cm$^2$, resulting in 95.5% and 99.2% of the fluence $7.84 \times 10^{17}$ D/cm$^2$. The amount at 300 K is nearly six times larger than that for 473 K. Thus, the amount is expected to be reduced largely at temperature nearly equal to or higher than that corresponding to the trap energy of defects. This difference is understood by estimating roughly the concentrations of mobile and trapped atoms at the temperatures illustrated in Figs. 2 and 4. Nearly the same ratio of retained amounts in polycrystalline tungsten at almost the same temperatures as cited above was also shown by an experiment and calculations for 200 eV $D^+$ ion fluence [8].

The depth profiles of deuterium atoms retained at 300 K are shown in Fig. 6 for fluences $4 \times 10^{15}$ D/cm$^2$, $7 \times 10^{17}$ D/cm$^2$ and $1.3 \times 10^{18}$ D/cm$^2$ corresponding to irradiation periods 2 s, 350 s, and 650 s. It is clear from Fig. 6 that, while the locations of their maxima did not move with time, the profiles were broadened out because of diffusion.

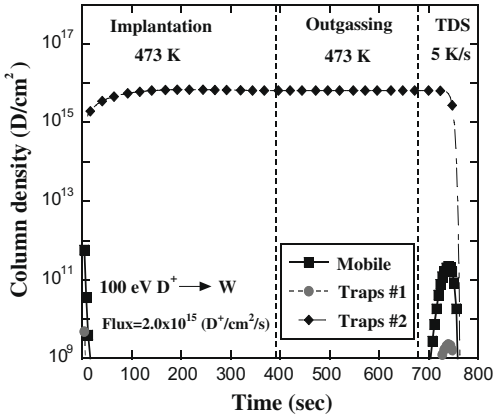


**Fig. 4.** Column density of mobile deuterium atoms and trapped atoms in trap #1 and trap #2 in the case of Fig. 3.

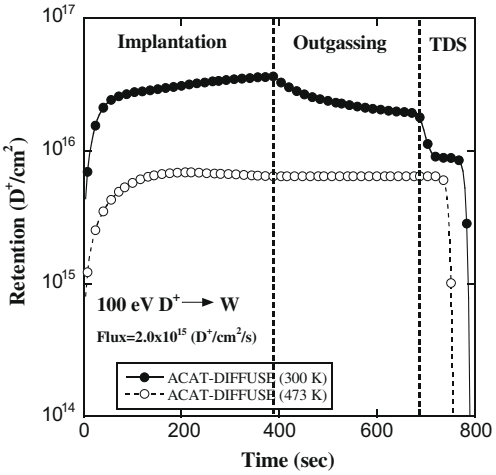


**Fig. 5.** Amounts of deuterium atoms retained at 300 K and 473 K in the first two periods.

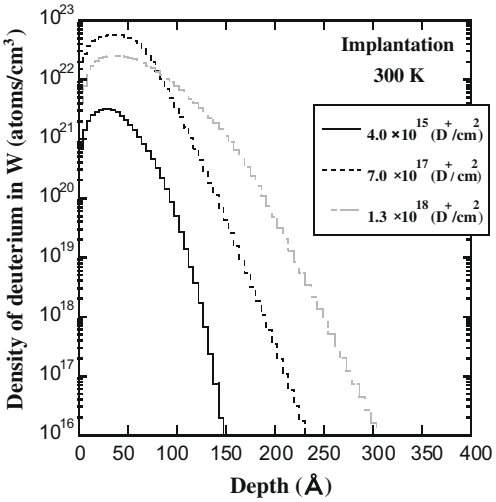


**Fig. 6.** Depth profiles of retained deuterium atoms for fluences $4 \times 10^{15}$ $D^+$/cm$^2$, $7 \times 10^{17}$ $D^+$/cm$^2$ and $1.3 \times 10^{18}$ $D^+$/cm$^2$ corresponding to irradiation periods 2 s, 350 s and 650 s.

## 4. Conclusion

With ACAT-DIFFUSE, we calculated fluxes of thermal $D_2$ re-emission, reflection and segregated self-sputtering of D from a $D^+$ implanted wrought tungsten material during a time sequence of l00 eV $D^+$ implantation, post-implanted isothermal out-gassing and thermal desorption spectroscopy. Diffusion was considered in the implantation period and radiation-enhanced effect was also considered in the damage range. The obtained result was in good agreement with the experiment by employing a diffusion coefficient of $1.0 \times 10^{-8} \exp(-0.39\ \text{eV}/kT)\text{cm}^2\ \text{s}^{-1}$, a recombination rate coefficient of $1.2 \times 10^{-25} \exp(+0.59\ \text{eV}/kT)T^{-1/2}\ \text{cm}^4\ \text{s}^{-1}$ and two trap sites with de-trapping energies of 0.85 eV and 2.2 eV and density fractions of 0.05 D/W and 0.01 D/W. The result suggests the existence of the two different trap sites in the material. Since the ACAT output indicated that vacancy was hardly created by 100 eV $D^+$ ions bombardment to the binary collision approximation, these trap sites may have previously been created before the experiment.

Only one TDS peak was seen in the calculated result for 473 K in the first two periods. So, the defects with de-trapping energy 0.85 eV were not capable of holding deuterium atoms at this temperature, indicating almost all atoms in the last two periods were trapped by traps with de-trapping energy 2.2 eV. The amount of deuterium atoms retained at 473 K was nearly six times smaller than that at 300 K. The amount of retained atoms is expected to be reduced largely for temperature nearly equal to the value corresponding to de-trapping energy of defects. The integrated fluxes released in the implanted period were estimated as $7.49 \times 10^{17}$ D/cm$^2$ and $7.78 \times 10^{17}$ D/cm$^2$, resulting in 95.5% and 99.2% of the fluence $7.84 \times 10^{17}$ D/cm$^2$.

The depth profiles of deuterium atoms retained in the implanted period showed that, while the location of their maxima for 300 K did not move with time, they were broadened out because of diffusion.

## Acknowledgements

The authors would like to thank Professor T. Tanabe, Professor K. Ohya and Professor Y. Ueda for their cooperation and discussions. This work was partly supported by KAKENHI (19055005).

## References

[1] ITER EDA Documentation Series, No. 7, IAEA (1996).
[2] G. Federici, R.A. Anderl, P. Andrew, et al., J. Nucl. Mater. 266–269 (1999) 14.
[3] A.A. Haasz, J.W. Davis, M. Poon, et al., J. Nucl. Mater. 258–263 (1998) 889.
[4] S. Nagata, K. Takahiro, J. Nucl. Mater. 283–287 (2001) 1038.
[5] A.A. Haasz, M. Poon, et al., J. Nucl. Mater. 290–293 (2001) 85.
[6] V.Kh. Alimov, K. Ertl, J. Roth, J. Nucl. Mater. 290–293 (2001) 383.
[7] M. Poon, R.G. Macaulay-Newcombe, et al., J. Nucl. Mater. 307–311 (2002) 723.
[8] O.V. Ogorodnikova, J. Roth, M. Mayer, J. Nucl. Mater. 313–316 (2003) 469.
[9] H.T. Lee, A.A. Haasz, J.W. Davis, et al., J. Nucl. Mater. 363–365 (2007) 469.
[10] R. Causey, K. Wilson, T. Venhaus, et al., J. Nucl. Mater. 266–269 (1999) 467.
[11] T. Venhaus, R. Causey, R. Doerner, et al., J. Nucl. Mater. 290–293 (2001) 505.
[12] V.Kh. Alimov, A.P. Zakharov, R.Kh. Zalavutdinov, in: A. Hassanein (Ed.), Hydrogen and Helium Recycling at Plasma Facing Materials, Kluwer Academic Publishers, 2002, p. 131.
[13] C. Garcia-Rosales, P. Franzen, H. Plank, et al., J. Nucl. Mater. 233–237 (1996) 803.
[14] P. Franzen, C. Garcia-Rosales, H. Plank, et al., J. Nucl. Mater. 241–243 (1997) 1082.
[15] J.P. Biersack, W. Eckstein, Appl. Phys. A 34 (1984) 73.
[16] Y. Yamamura, Nucl. Instr. Meth. B 28 (1987) 17.
[17] Y. Yamamura, Y. Mizuno, IPPJ-AM-40, Institute of Plasma Physics, Nagoya University (1985).
[18] K.L. Wilson, M.I. Baskes, J. Nucl. Mater. 76&77 (1978) 291.
[19] K.L. Wilson, Nucl. Fusion (1984) 28. Special Issue.
[20] M.A. Pick, K. Sonnenberg, J. Nucl. Mater. 131 (1985) 208.
[21] R. Frauenfelder, J. Vac. Sci. Technol. 6 (1969) 388.